Dependence of Wear and Mechanical Behavior of Nitrocarburized/CrN/DLC Layer on Film Thickness

Fábio Faria Conde[a]* [iD], Julian Arnaldo Ávila Diaz[b] [iD], Guilherme Faria da Silva[c] [iD],

André Paulo Tschiptschin[c]

[a]*Departamento de Materiais, Universidade de São Paulo, Av. João Dagnone, 25, CEP 13568-250, São Carlos, SP, Brasil*
[b]*Universidade Estadual Paulista - UNESP, Av. Profª Isette Corrêa Fontão, 505, CEP 13876-750, São João da Boa Vista, SP, Brasil*
[c]*Departamento de Engenharia Metalúrgica e de Materiais, Universidade de São Paulo, Av. Prof. Mello Morais, 2463, CEP 05508-030, São Paulo, SP, Brasil*

Diamond-like carbon (DLC) films are amorphous metastable carbon form that provide interesting mechanical and tribological properties. The role of film thickness influence upon wear and mechanical properties is of interest and not yet fully reported. In this study, two samples of previously plasma nitrocarburized, quenched and tempered H13 steel were duplex treated. First, a physical vapor deposition (PVD) chromium nitride (CrN) layer was applied, followed by a top final diamond-like carbon layer applied by plasma-enhanced chemical vapor deposition (PECVD). To evaluate thicknesses influence on mechanical and wear properties of coatings, samples were treated using two different thicknesses of both layers. In this study, the thickest CrN and DLC case presented higher hardness and better tribological properties, however, its failure occurs in brittle fashion.

Keywords: *Duplex coatings, DLC coating, CrN coating, wear, PECVD.*

1. Introduction

Diamond-like carbon (DLC) is a metastable form of carbon, containing sp³ diamond bonds, sp² graphite bonds and sp² chain bonds, hence, DLC coatings can present high mechanical hardness, good chemical inertness and great tribological properties [1]. DLC also contains a percentage of hydrogen, originating the so-called aC:H, amorphous hydrogenated carbon alloys [1]. Coating-substrate material adhesion is one a key issue for wear resistant coatings. Wear of a hard coating usually starts with formation of microcracks that cause spalling of the superficial layer, mainly at surface asperities [2]. Thin coatings are reported in the literature as being smaller than 1µm [1,3], even with applications that requires sub-100 nm thickness. In general, thin and very thin DLC coating tend to present brittle behavior and high hardness. Meanwhile, thick coatings are categorized above 10 µm [1,4,5]. Due to the high internal compressive stress of DLC film, to deposit a thick DLC film it is necessary to add different elements to the DLC coating, as Si for instance, to reduce internal stress [4,5], causing a reduction on hardness (doped or alloyed DLC).

Under high loading conditions, a thin coating may collapse, mainly due to substrate elastic and plastic deformations, resulting in premature failure of the coating. Very thin coatings may be undesired because of higher susceptibility of substrate influence. On the other hand, excessive thick coatings diminishes internal residual stress of the film and lowers adhesion to the substrate, resulting in poor mechanical and wear properties [1,3]. For many applications, coating performance is limited by the mechanical properties of the substrate material, so smooth hardness gradients are desirable for better coating adherence and can be achieved by previous treatments, hardening the substrate and improving wear lifetime [2,6]. Thus, deposited films require mechanical support to be provided by the substrate material, granting good adhesion and avoiding the so-called "eggshell effect" [6,7]. Hardness gradients built-up by duplex treatments is common to ensure good adhesion, and plasma nitriding has been reported as a load carrying improving treatment, providing a better support to hard and brittle coatings [7-12].

Ni interlayer and its thickness affect the growth of DLC films, thicker Ni interlayer promoted higher growth than thin interlayer on DLC film, then Ni interlayer can act as a catalytic environment for DLC growth [13]. Thick DLC films are generated when thicker interlayer are deposited, however, thick DLC films presented higher surface roughness and friction coefficient than thin films [13]. A similar result was reported using Cr as interlayer [14], presenting a not linear correlation between interlayer thickness and DLC thickness. Therefore, soft film are produced from the onset where the film gets thick enough to lower hardness and wear properties [13-15].

The correct interlayer distribution and DLC film thickness results on a hard coatings. Dorner et al. [15] studied three thickness of DLC film, 0.7 µm, 1.5 µm and 3.0 µm.

*e-mail: fabiofariaconde@gmail.com

For all conditions hard and brittle case were generated, being reported good adhesion and similar wear resistance independent of film thickness. The scratch tests depicted similar critical loads, with only significant difference at the spalling between different DLC film thicknesses, as the thickest one presented extensive spalling, forming a larger crack net than the thinnest film [15]. In addition, the thickest film presented adhesive failure, leaving DLC detached particles on scratch path, concluding that thin DLC coating present a better wear resistance [15]. Shahsavari et al. [14] performed several scratches tests, obtaining a plastic pattern of deformation for thicker DLC film conditions, presenting a blister which was reported as poor wear behavior and adhesion of the film.

Thick films, ranging between 0.03 nm to 5.0 nm, presented high critical load, high coefficient of friction and increase of wear depth, presenting inflections in some cases [16,17]. On the other hand, DLC coatings with thickness from 10 nm to 2000 nm showed an exponential decrease of wear with the film thickness decreasing [18], thus, high loads produces low wear. A similar trend was reported on coatings with thicknesses between 60 nm to 300 nm, resulting in high surface roughness and low critical loads as the film thickness increased [19]. Additionally, the coefficient of friction suffers a decreasing trend as thickness increases, as well as number of sliding laps increases [19]. Moreover, coefficient of friction also showed dependence with applied force, resulting in low coefficient of friction for thick films when applied low loads, and low coefficient of friction for thin films when applied high loads [20]. Varying thickness from 5.6 nm up to 85 nm, a maximum hardness condition was achieve at 46 nm film thick [20]. Overall, there is a great dependence of tribological and mechanical properties on film thickness.

The role of the CrN and DLC film thicknesses on the mechanical and tribological properties of coatings is here studied. DLC can present high hardness, therefore, several treatments were required to guarantee smooth hardness gradient and good adherence to a bare quenched and tempered H13 tool steel. Thus, to avoid numerous depositions in this study, a previous AISI H13 tool steel thermochemically treated (quenched, nitrocarburized and tempered) was used as the substrate material. Following the nitrocarburization treatment, two films (~1-3μm), CrN and DLC, with different thicknesses, were deposited by PVD and PECVD processes, respectively. A correlation between CrN and DLC film thicknesses, mechanical properties, wear and adhesion to the substrate were made. Wear tests results were also compared with those obtained for the simply nitrocarburized H13 tool steel. Light optical microscopy, scanning electron microscopy, Raman spectroscopy and nanohardness indentation were performed for microstructural characterization. Wear tests, scratch tests and Rockwell C adhesion tests were carried out for wear assessment.

2. Experimental

Samples of a quenched AISI H13 steel were ground and prepared according to ASTM E3 standard [21], grounded from mesh 80 to 2000, and polished with chromium oxide. Plasma nitrocarburizing treatment was conducted in these polished samples. Initially, an argon sputtering was carried out to clean the chamber and the samples during 1 hour at 400°C. Subsequently, a nitrocarburizing procedure was carried out at 550°C, for 5 hours, using a 77% H_2, 20% N_2, 3% CH_4 precursor gas, at 6 mbar. The applied electric current was 800 mA, under a 3 kHz pulsed 590 V applied voltage, with a 92% duty cycle. Hardness was measured before and after nitrocarburizing.

A layer of CrN was deposited on the nitrocarburized surface, via PVD. Different times of CrN deposition were used to obtain different thicknesses. Afterwards, DLC layer was deposited using the PECVD at 180°C. DLC thickness increase was according to CrN increased layer thickness, as reported in previous studies [13,14].

Argon gas was used for sputtering (cleaning) and acetylene as precursor gas for the DLC deposition. Processing temperature was 180ºC and the deposition time was 10 h, as depicted in Table 1. Two different depths of prior CrN and final DLC layers were deposited. Two samples were used to evaluate the thicknesses influences on the mechanical and tribological properties.

These samples were cut, mounted and their cross sections characterized by scanning electron microscopy. Raman spectroscopy was carried out to characterize the amount of sp^2 and sp^3 bonds present in the DLC layers.

Wear tests were carried out using a fixed rolling sphere method without the use of an abrasive, as proposed by Rutherford et al. [22]. A quenched 52100 bearing steel, 60 HRC hard, 25.4 mm in diameter was used as the sphere, rotating at 250 RPM. 0.85 and 2.25 N loads were applied, with total testing times of 40 and 60 minutes, respectively. The total wear volume (V) was calculated with equation 1 and 2 through the relationship of cap diameter (d), height of material removed (h) and original ball radius (r) according to ASTM G99-17 [23].

$$h = r - \sqrt{\left[r^2 - \left(\frac{d^2}{4} \right) \right]} \quad \text{(Equation 1)}$$

$$V = \left(\frac{\pi h}{6} \right) \cdot \left(\frac{3d^2}{4 + h^2} \right) \quad \text{(Equation 2)}$$

Nanohardness measurements, according to ASTM E2546-07 [24], were performed using TriboIndenter, using a Berkovich type diamond tip. A total of 25 indentations on each sample were performed using a 5,000 (N load in a single test cycle at room temperature (23° C). The penetration

Table 1. Deposition of interlayer and final coating parameters.

	CrN interlayer	DLC coating
Method	PVD	PECVD
Temperature	150-200°C	180°C
Pressure	10E-1 Torr	5 Torr
Deposition time	Depends on thickness	10h
Gas	Ar	C2H2

depth during testing did not exceed 120 nm, less than 7% of the DLC layer thicknesses.

A good adherence of the coating to the substrate is required to grant good wear and friction behaviors. Lack of adhesion may allow the formation of interfacial cracks, causing premature failure. Scratch tests are commonly used to evaluate the adhesion between the deposited coating and the substrate. Scratch tests were carried out according to ASTM C1624-05 standard [25] , using a universal tribometer, with normal progressive force, ranging from 2 to 80 N, at a rate of 50 N min^{-1}. A 120º conical Rockwell C indenter with a 200 µm tip radius was used in this set of testing, with 3 tests conducted on each sample.

An additional adhesion test was carried out, using the modified Daimler indentation test, according to VDI 3198 [26], by applying a 1,471 N load on a conical Rockwell C indenter with 200 µm tip radius, and comparing the crack pattern after unloading with quality indexes given by the standard. Rockwell C adhesion test consists in a method of checking the adhesion of PVD coatings that relies on observation of a Rockwell C indent. The stresses around the rim of a normal Rockwell C indent may cause microcracking and delamination of the coating. Thereafter, the greatest stresses at the rim of the crater taper off radially outward the coating, and this affected area gives an indication of the adhesion of the coating. A set of 6 standard drawings is used to classify the indent as a measurement value [26].

3. Results

3.1 Micrographs

Figure 1 shows the cross-section of the nitrocarburized AISI H13 steel with an intermediate PVD deposited CrN
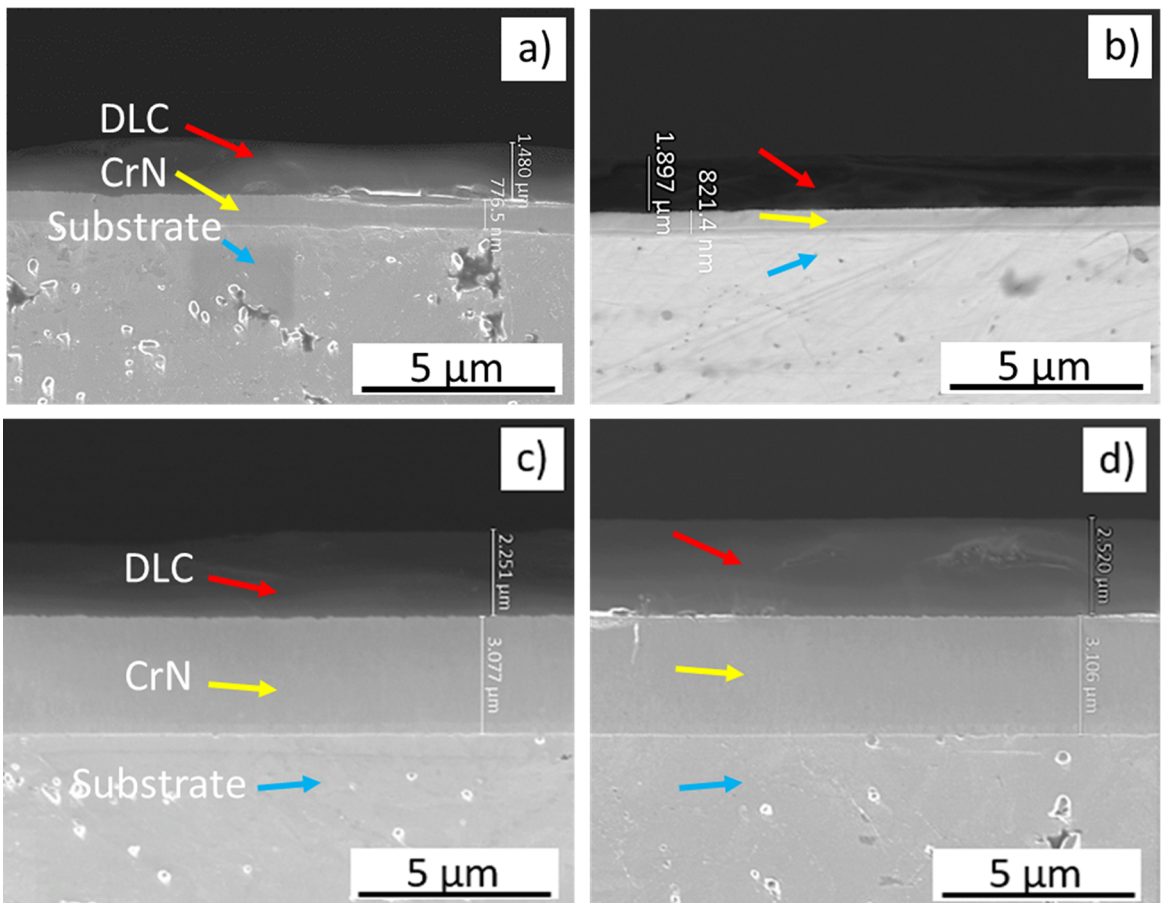

Figure 1. SEM images of the cross sections of the coated samples, a) and b) DLC-1, c) and d) DLC-2. Red, yellow and blue arrows indicate DLC coating, CrN chromium nitride interlayer and the PNC- plasma nitrocarburized substrate, respectively.
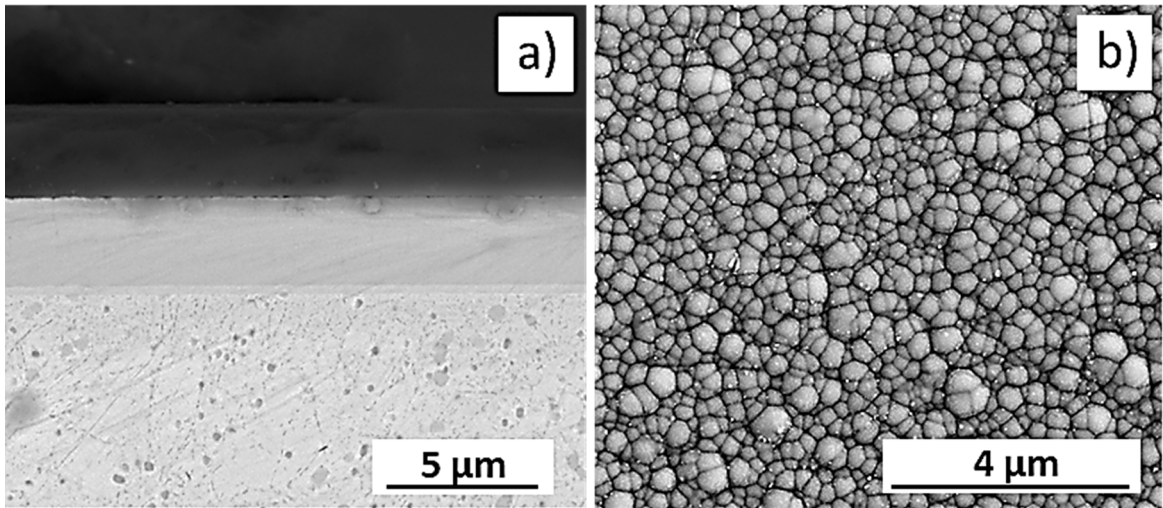
Figure 2. SEM image of the a) film cross section, b) top view.

layer and an outermost PECVD deposited DLC layer samples. DLC-1 sample presented a 0.80±0.17 µm thick intermediate CrN layer and a 1.65±0.19 µm thick final DLC coating. The DLC-2 sample presented a 3.11±0.05 µm thick CrN layer and a 2.43±0.11 µm thick outermost DLC layer. Figure 1a and 1b shows the microstructure of the cross section of the DLC-1 sample and Figure 1c and 1d the microstructure of the cross section of the DLC-2 sample. Figure 2 depicted faultless DLC layers, presenting no pores or defects in the cross-section. Also, its top view reveals a globular growth, as reported [13,27,28]

3.2 Raman spectroscopy

Raman spectroscopy curves are presented in Figure 3, with presence of the two main peaks, D and G. Both DLC-1 and DLC-2 depicted wide bands with peaks centered in the region of the bands D and G of graphite, due to the high degree of crystallographic disorder. The larger the Raman spectrum line, the more amorphous the material is, which is explained by less coherency of the photons scattered during the Raman process due to the lack of crystallinity [1]. D peak usually appears at 1350 cm^{-1} and represents the breathing vibration mode of disordered graphite, meaning graphite presence [1]. G peak, around 1580 cm^{-1} is sensitive to all sp² sites vibrations, whether in aromatic rings or chains. The I (D) / I (G) ratio obtained from the Raman analyses gives a good indication of the presence of more aromatic films. Lower ratio values means the presence of less aromatic rings inside the film instead of sp² or sp³ chain bonds [1]. Samples presented a very close I (D) / I (G) ratio, respectively 0.700 to 0.723 for DLC-1 and DLC-2, indicating a disordered amorphous structure containing sp2 and sp3 bonding. The higher I(D) / I (G) found in the DLC-2 coating suggests higher graphite formation in the DLC-2 coating.

3.3 Hardness

The quenched hardness of the H13 steel was 580 ± 10 Vickers. The nitrocarburized case was 100 µm deep and 950 ± 17 Vickers. Nanohardness, Young moduli and depth

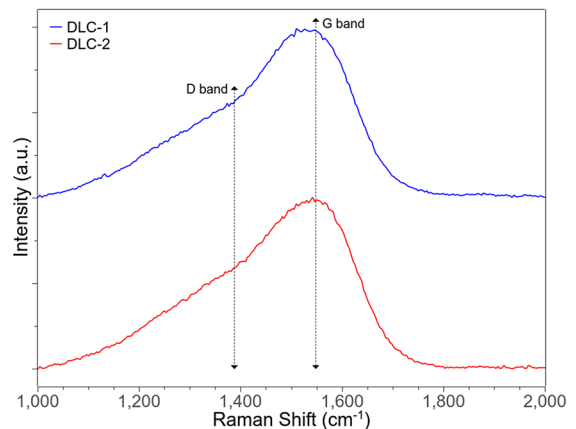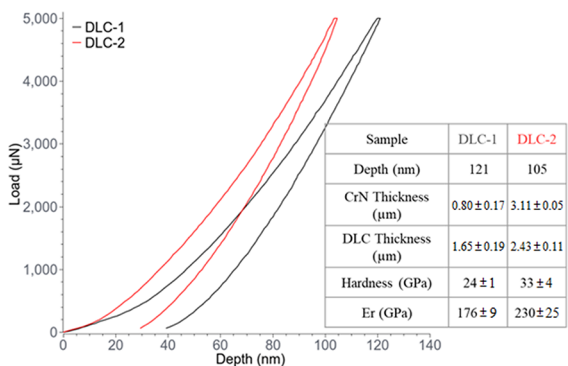**Figure 3.** Raman spectroscopy highlighting D and G peaks as function of carbon bonds.

Sample	DLC-1	DLC-2
Depth (nm)	121	105
CrN Thickness (µm)	0.80±0.17	3.11±0.05
DLC Thickness (µm)	1.65±0.19	2.43±0.11
Hardness (GPa)	24±1	33±4
Er (GPa)	176±9	230±25

Figure 4. Load-displacement curves for DLC-1 and DLC-2 coatings.

of indentation of the DLC coatings were assessed through a one-cycle nanohardness testing with 13 seconds dwell time (Figure 4). DLC-1 sample is thinner and presents lower hardness and elastic modulus than DLC-2.

3.4 Wear test

A set of tests were performed applying 0.85 N and 2.25 N load for DLC-1 and DLC-2 samples. The wear tests were interrupted at 5 min, 10 min, 15 min, 20 min and 40 min for the 0.85 N load and an additional time of 60 minutes for the 2.25 N load.

As shown in Figure 5, samples DLC-1 and DLC-2 showed better performances, with much less volume loss than the just nitrocarburized Q&T H13 steel. Notice also that, for the DLC-1 sample, the 2.25 N test load worn the DLC film completely, reaching the chromium nitride intermediate layer while, in the case of the DLC-2 thicker coating, the intermediate CrN layer was not exposed.

Some craters after the wear test are shown in Figure 6 and Figure 7. Diameters of wear craters of 500 µm, 400 µm and 900 µm, for DLC-1, DLC-2 and the uncoated AISI H13 steel, respectively. The wear crater formed on the nitrocarburized Q&T H13 sample reached the substrate under both applied load cases. For the 2.25N applied load, the nitrocarburized layer was totally worn between 40 and 60 minutes, equivalent to 800 to 1200 m, increasing the wear as shown in Figure 5 (b).

Wear mechanisms of adhesion predominated in early stages, accompanied by three-body abrasion. As CrN was exposed, two-body abrasion wear mechanism was activated, increasing wear rate. A result summary in Table 2 is presented as following.

3.5 Scratch Test

Figure 8a and 8b show the result of a scratch test carried out on the surface of specimen DLC-1. The normal load (Fz) was increased linearly from 2 N to 80 N, black line. Acoustic emission (AE), red line, was monitored in order detect the formation of the first cracks in the DLC film. The blue line (CoF) indicates the apparent coefficient of friction between the diamond indenter and the DLC-film.

The scratch tests results reveal the first critical failure loads (Lc1) of 49 and 51 N, for the DLC-1 and DLC-2, respectively, corresponding to nucleation of the first tiny
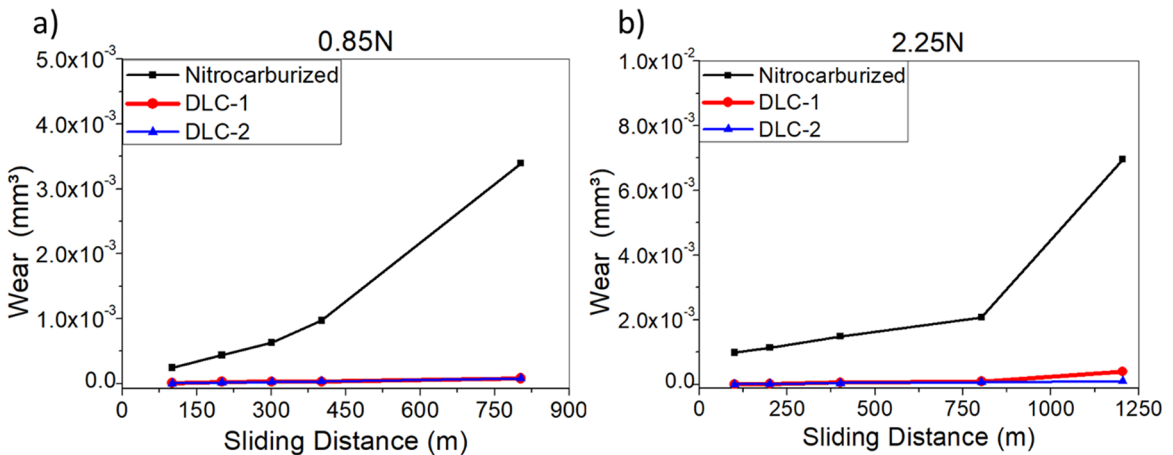

Figure 5. Sliding sphere wear test in the nitrocarburized condition and after DLC deposition, a) load of 0.85N and b) 2.25N.
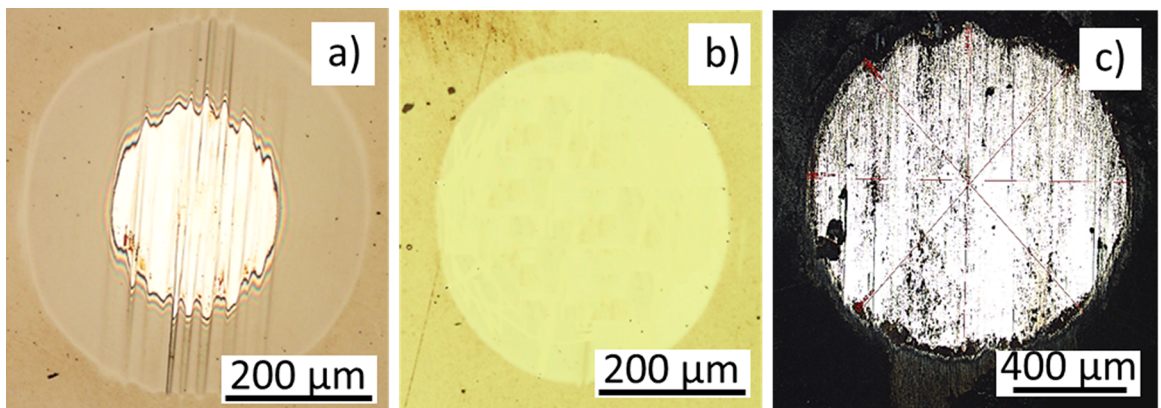

Figure 6. Wear craters formed during wear tests conducted under 2.25 N, 250 RPM, 60 minutes, a total distance of 1197 meters. a) DLC-1: 500 µm wear crater, with exposure of the CrN intermediate layer, after removal of the DLC film; b) DLC-2: 400 µm wear crater, still showing the DLC coating; c) nitrocarburized Q&T H13 steel: 900 µm wear crater showing the exposed H13 substrate.
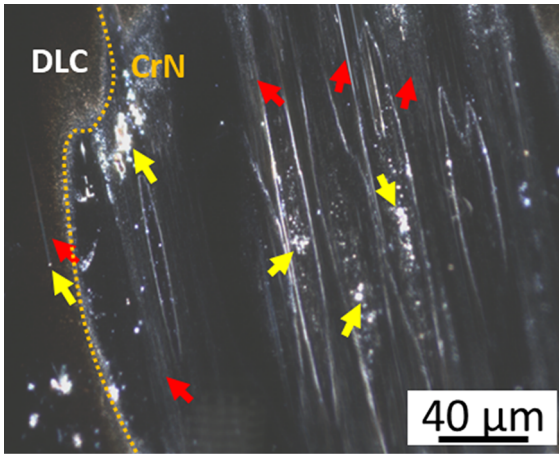
Figure 7. DLC-1 Wear cap, after wear test. Yellow arrows show adhesive wear and red arrows show abrasive wear.

cracks at 45° relative to the sliding direction. The second critical load (Lc2) could not be detected in both scratch tests, carried out under loads up to 80 N. Higher AE value and AE oscillation is observed on DLC-2 because of the high hardness, so when film delaminates, high energy is released in sound form. Also, DLC-2 presented lower apparent CoF than DLC-1.

Figure 9a and 9b show the mid-length appearance of the scratches made on the surface of DLC-1 and DLC-2 coatings. Figure 10a and 10b show the end regions of the scratches and 10c and 10d all length after Lc1 scratching. Very small spallation regions initiating at the border of the scratch are depicted with few heavy spallation after Lc1 for DLC-2.

Scratching tests shows that both DLC-1 and DLC-2 duplex coatings presented very good adhesion, with Lc1 critical loads for initiation of the first tiny cracks at the border of the scratch of 49 and 51 N, respectively. No Lc2, corresponding to film continuous spallation was observed. These results can be compared to other studies published in literature reporting critical failure loads of DLC films deposited on 304L austenitic stainless steel of 24 N using the same Rockwell-C indenters with 0.2 mm tip radius [6]. Both analyzed duplex coatings presented good results, the thicker DLC-2 coating being a little bit better than the thinner DLC-1, with higher Lc1 - critical load and lower apparent coefficient of friction, of 0.07 to 0.16 for the DLC-1 coating and 0.03 to 0.13 for the DLC-2 below Lc1 regime, indicating that harder coatings result in lower coefficient of friction. Both DLC-1 and DLC-2 layers presented a very low coefficient of friction and this is one of DLC films main characteristics.

During scratching test when Lc1 is reached, cracks start to propagate in the DLC coating in a brittle fashion, causing its failure. Despite this, the small cracks did not propagate circularly, as reported by Zaidi et al. [29] leading to spalling of the DLC coating very similar to the spalling observed in bulk glass. On the contrary, most of the tiny cracks formed
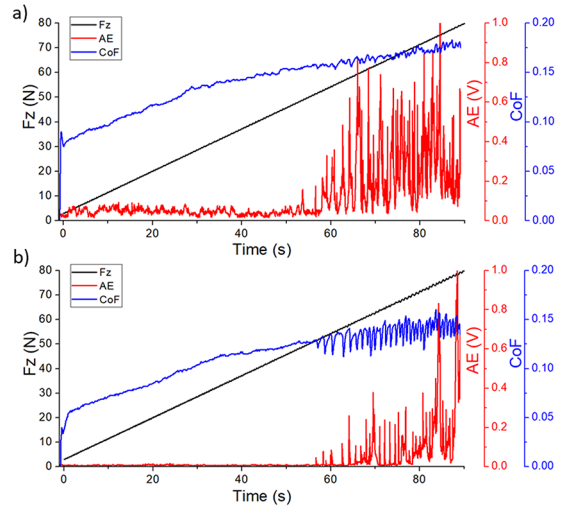

Figure 8. Results of scratch test carried out on DLC-1 and DLC-2 coatings. Fz (black), AE (red) and CoF (blue) signals are indicated. (a) DLC-1 coating starts failing at a 49 N Lc1 critical load. (b) DLC-2 coating starts failing at a 52 N Lc1 critical load for the formation of the first cracks. CoF varies from 0.08 to 0.15.
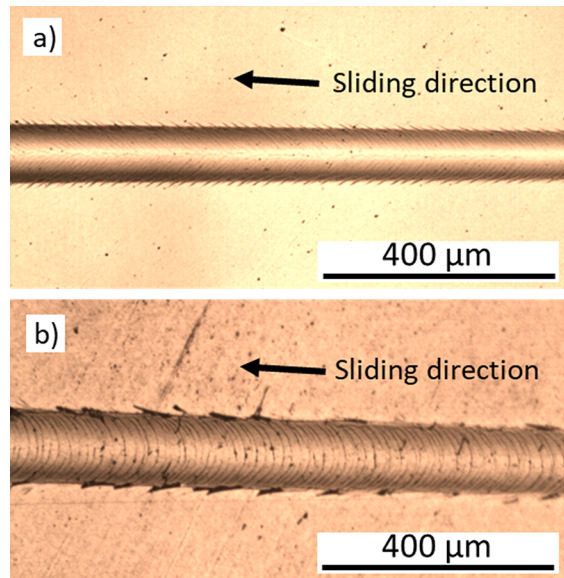

Figure 9. Image of the scratch taken at the mid length of the total scratch showing that the DLC film was not removed. Small cracks can be seen at the bottom of the scratch forming ~45° with the sliding direction. a) DLC-1, b) DLC-2.

Table 2. Results summary

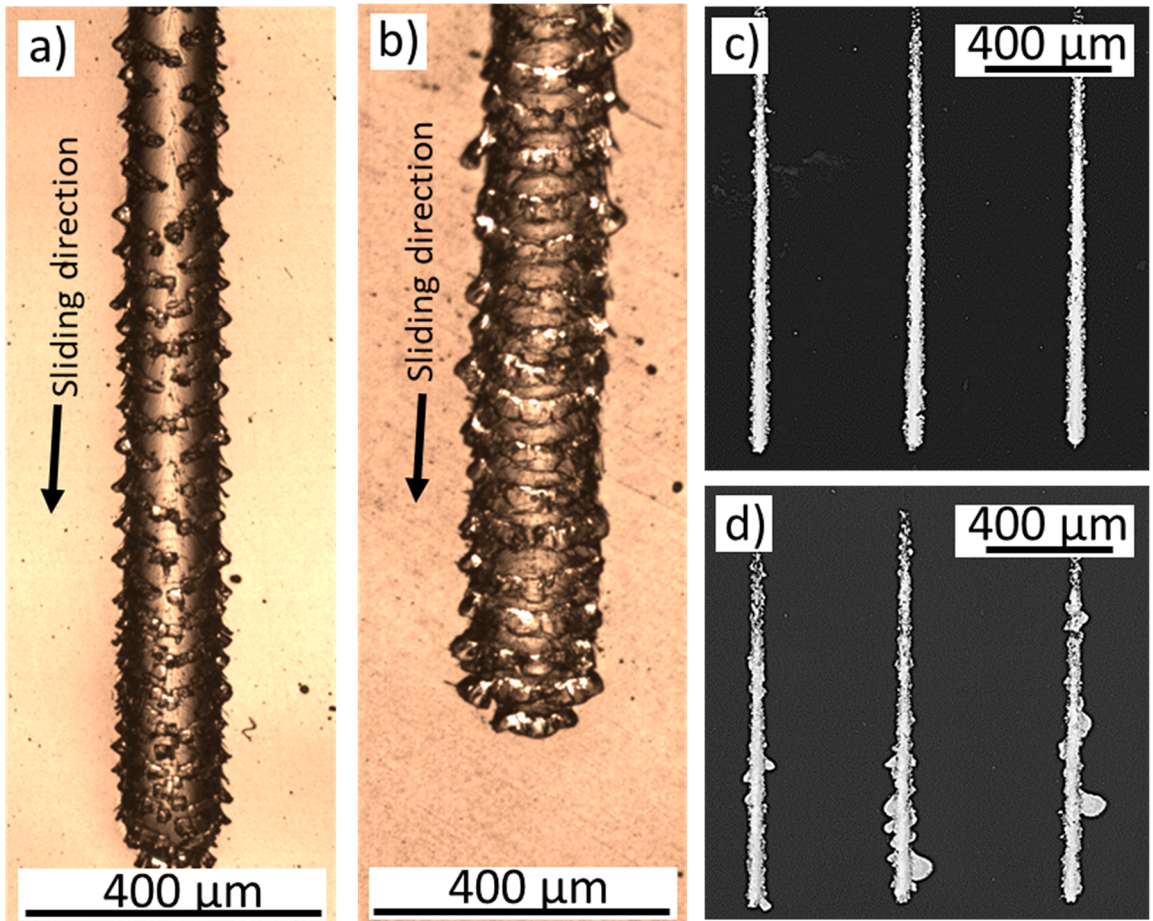| Sample	Cr thickness	DLC thickness	I(D)/I(G)	Hardness	Wear Rate (2.25N*)	Critical Load
DLC-1	0.8 μm	1.65 μm	0.7	24 GPa	6.77E-17 m³/N·m	49 N
DLC-2	3.11 μm	2.43 μm	0.723	33 GPa	3.88E-17 m³/N·m	51 N

Figure 10. Image taken from the end of the scratch, showing that the DLC film was not removed under an applied load of 80 N. Small spallation regions can be seen propagating from the borders of the scratch, forming ~45º with the sliding direction. a, c) DLC-1 and b, d) DLC-2.

on the border of the scratch, at 45º with the sliding direction, stopped growing once the concentrated load decreased after the passage of the indenter. Only on DLC-2 some spallation and side material detachment is observed in some spots as shown in Figure 10d.

Friction force oscillation is caused by the succession and alternation of stages between indenter contact against coating layer, increase of contact pressure, microcrack propagation followed by coating delamination and drop of contact pressure. It can be noticed, because of higher DLC-2 hardness, higher forces must be produced to advance the indenter. Once it reaches a limit, microcracks are propagated causing spalling. This material removal in front of the indenter results in a drop of instantaneous force, causing pop ins.

3.6 Rockwell C indentation tests

Figure 11 shows images of the surface of the indentation made during a Rockwell C adhesion test (Daimler Benz test) [26] carried out using a diamond cone indenter, 200 μm tip radius, under an applied load of 1471 N on the DLC-1 and DLC-2 coated surfaces. Once the load has been removed, the surface of the

specimen was observed in an optical microscope in order to classify the coating adhesion as HF 1 to HF 6 according to the amount of cracking or spallation around the indent, as reported in VDI 3198 standard for coating assessment [26].

Good adhesion and absence of delamination depicted on Rockwell C indentation test, of samples previously nitrocarburized, submitted to PVD deposition of CrN (duplex treatment) and PECVD deposition of DLC, granted good mechanical support. A smooth transition between the Q&T substrate and the DLC aid avoiding an "eggshell effect", despite presented layer thickness. Rockwell C indentation test confirms good adhesion, classifying the studied coating as HF-1, and once adhesion is good, the wear and spalling takes much longer to occur.

4. Discussion

Wear test showed good improvement on component lifetime for DLC coated samples compared to the Q&T H13 specimen as shown in Figure 5. Also, both DLC-1 and DLC-2 resulted in very close wear rate and DLC-1 got
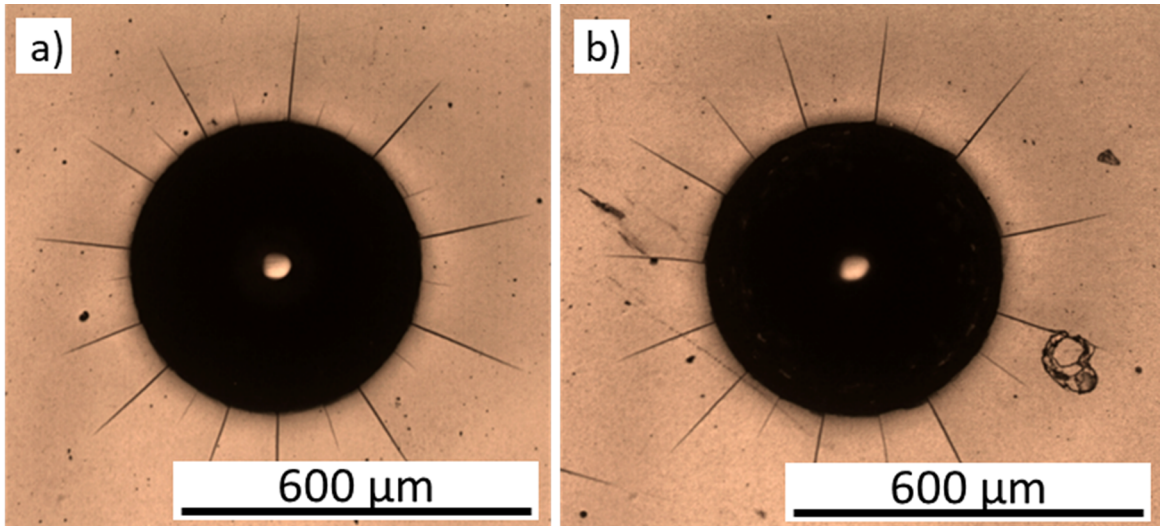
Figure 11. Images of the indented surface showing only radial cracks, classified as HF-1: (a) DLC-1 and (b) DLC-2. No spalling was observed.

exposed earlier because of a thinner deposited film. The initial wear mechanism on wear test was mainly adhesive, through galling and cracking of superficial material, removing small pieces of material. These loosen particles started to act as abrasive, scratching the tested specimen, initiating a three-body abrasive wear mechanism along the DLC coating. These particles did not adhere to the sliding ball because of low chemical affinity and lack of plasticity, which provides an excellent galling resistance [30]. Once wear reached the CrN intermediate layer, CrN was able to adhere to the sliding ball and act as a rigid anchorage for the DLC fragments. In this stage, two-body microabrasive and microploughing wear regimes predominated. Figure 6 shows the abrasive mechanism by highlighting ploughing lines formed only along the width of the exposed CrN wear track (Figure 6a); near the edges of the exposed CrN the formed ploughs are less intense, suggesting that it has shortly started because CrN layer just got exposed. Figure 6a shows wear test cap revealing adhesive wear on DLC and abrasive wear mainly on the exposed CrN due to removed CrN material acting as anchorage for DLC fragments. In addition, Figure 6c exhibits nitrocarburized H13 higher material removal by combination of adhesive and abrasive wear, exposing H13 substrate. Similar description is made in other studies where brittle particles penetrate DLC, causing small detachments and these new free particles act as abrasive as well [10,15]. Therefore, once substrate is reached, wear rate will present a significant increase.

Scratching analysis corroborates with the hardness once the acoustic emission of DLC-2 sample has higher values compared to DLC-1. This demonstrates brittle character of rupture due to greater hardness of DLC-2 sample, producing higher acoustic emissions. It has been reported that harder substrates show better adhesion and produces higher acoustic emission when film delamination occurs [31].

Conversely, it was reported that thinner layers presented lower sliding wear rates as well as higher interface adhesion [32,33]. It is important to point out that hardness is the main parameter to determine adhesion and wear. In both studies [32,33] it was also presented among the studied samples a thicker layer with higher hardness than a thinner layer, that resulted in better wear resistance and interface adhesion. The present work discusses the difference between two CrN/DLC multilayer concerning tribologic and mechanical properties as a function of layer thickness. As expected, the thickest one was the hardest layer, presenting lower wear rate, higher critical load for spallation, higher elastic modulus and lower apparent coefficient of friction.

Furthermore, it is likely that, between two different layer thickness but considering similar composition and mechanical properties, the thicker one would last long to wear and reach substrate because of its size. However, changing thickness of films also change several properties along. It is important to highlight that thinner layers may present the "eggshell" effect, due to the high residual stress and intense gradient of mechanical properties. In addition, considering the recommendation of not exceeding a penetration/deformation deeper than 10% to avoid substrate influence, it is important to notice that thinner layers at a certain size would produce little or no improving effect on the substrate as the 10% layer thick would just be too small, becoming merely insignificant.

5. Conclusions

1. Despite the thickness difference of CrN and DLC layers, both coatings presented good adhesion according to Daimler Benz test classified as HF-1.

2. In this study, the thicker CrN interlayer promoted the growth of a thicker DLC film. Also, the thicker CrN and DLC layer decreased more the influence of substrate and preserved the compressive stress inherent of DLC film, presenting higher hardness and better wear resistance.

3. Both DLC coatings presented low coefficient of friction measured during linear scratch tests. However, the harder DLC coating presented failure in brittle fashion, and showed few spallation during scratching test. Both coatings presented high critical loads during scratching test (49 and 51N).

4. Nitrocarburizing followed by duplex coating, consisting of PVD deposited CrN layer, followed by PECVD DLC layer, resulted in a significant improvement in wear-lifetime compared with the nitrocarburized H13 tool steel.

6. Acknowledgments

7. References

1. Robertson J. Diamond-like amorphous carbon. *Materials Science and Engineering: R: Reports*. 2002;37(4-6):129-281. DOI: 10.1016/S0927-796X(02)00005-0

2. Psyllaki PP, Jeandin M, Pantelis DI, Allouard M. Pin-on-disc testing of PE-CVD diamond-like carbon coatings on tool steel substrates. *Surface and Coatings Technology*. 2000;130(2-3):297-303.

3. Charitidis CA. Nanomechanical and nanotribological properties of carbon-based thin films: A review. *International Journal of Refractory Metals and Hard Materials*. 2010;28(1):51-70. DOI: 10.1016/j.ijrmhm.2009.08.003

4. Takeuchi S, Tanji A, Miyazawa H, Murakawa H. Synthesis of thick DLC film for micromachine components. *Thin Solid Films*. 2004;447-448:208-211. DOI: 10.1016/S0040-6090(03)01058-7

5. Dalibón EL, Escalada L, Simison S, Forsich C, Heim D, Brühl SP. Mechanical and corrosion behavior of thick and soft DLC coatings. *Surface and Coatings Technology*. 2017;312:101-109. DOI: 10.1016/j.surfcoat.2016.10.006

6. Recco AAC, Tschiptschin AP. Structural and Mechanical Characterization of Duplex Multilayer Coatings Deposited onto H13 Tool Steel. *Journal of Material Research and Technology*. 2012;1(3):182-188. DOI: 10.1016/S2238-7854(12)70031-5

7. Tschiptschin AP. Duplex Coatings. In: Wang QJ, Chung YW, eds. *Encyclopedia of Tribology*. Boston: Springer; 2013. p. 794-800. DOI: 10.1007/978-0-387-92897-5

8. Podgornik B, Vižintin J, Wänstrand O, Larsson M, Hogmark S, Ronkainen H, et al. Tribological properties of plasma nitrided and hard coated AISI 4140 steel. *Wear*. 2001;249(3-4):254-259. DOI: 10.1016/S0043-1648(01)00564-6

9. Sharma N, Kumar N, Dash S, Das CR, Subba Rao RV, Tyagi AK, et al. Scratch resistance and tribological properties of DLC coatings under dry and lubrication conditions. *Tribology International*. 2012;56:129-140. DOI: 10.1016/j.triboint.2012.06.020

10. Dalibon EL, Trava-Airoldi V, Pereira LA, Cabo A, Brühl SP. Wear resistance of nitrided and DLC coated PH stainless steel. *Surface and Coatings Technology*. 255:22-27. DOI: 10.1016/j.surfcoat.2013.11.004

11. Dalibón EL, Heim D, Forsich C, Rosenkranz A, Guitar MA, Brühl SP. Characterization of thick and soft DLC coatings deposited on plasma nitrided austenitic stainless steel. *Diamond & Related Materials*. 2015;59:73-79. DOI: 10.1016/j.diamond.2015.09.010

12. Kovacı H, Baran Ö, Yetim AF, Bozkurt YB, Kara L, Çelik A. The friction and wear performance of DLC coatings deposited on plasma nitrided AISI 4140 steel by magnetron sputtering under air and vacuum conditions. *Surface and Coatings Technology*. 2018;349:969-979. DOI: 10.1016/j.surfcoat.2018.05.084

13. Shahsavari F, Ehteshamzadeh M, Eslami PA, Irannejad A. Thickness evolution of nickel nano layer on the microstructure and adhesion strength of DLC films. *Studia Universitatis Babes-Bolyai Chemia*. 2016;61(1):107-114.

14. Shahsavari F, Ehteshamzadeh M, Naimi-Jamal MR, Irannejad A. Nanoindentation and nanoscratch behaviors of DLC films growth on different thickness of Cr nanolayers. *Diamond & Related Materials*. 2016;70:76-82. DOI: 10.1016/j.diamond.2016.10.003

15. Dorner A, Schürer C, Reisel G, Irmer G, Seidel O, Müller E. Diamond-like carbon-coated Ti6Al4V: influence of the coating thickness on the structure and the abrasive wear resistance. *Wear*. 2001;249(5-6):489-497.

16. Miyake S, Inagaki J, Miyake M. Dependence of the friction durability of extremely thin diamond-like carbon films on film thickness. *Wear*. 2016;356-357:66-76. DOI: 10.1016/j.wear.2016.02.016

17. Miyake S, Yamazaki S. Nanoscratch properties of extremely thin diamond-like carbon films. *Wear*. 2013;305(1-2):69-77. DOI: 10.1016/j.wear.2013.05.005

18. Wilson GM, Sullivan JL. An investigation into the effect of film thickness on nanowear with amorphous carbon-based coatings. *Wear*. 2009;266(9-10):1039-1043. DOI: 10.1016/j.wear.2008.12.001

19. Khun NW, Liu E. Investigation of structure, adhesion strength, wear performance and corrosion behavior of platinum/ruthenium/nitrogen doped diamond-like carbon thin films with respect to film thickness. *Materials Chemistry and Physics*. 2011;126(1-2):220-226. DOI: 10.1016/j.matchemphys.2010.11.036

20. Ma XG, Komvopoulos K, Wan D, Bogy DB, Kim YS. Effects of film thickness and contact load on nanotribological properties of sputtered amorphous carbon thin films. *Wear*. 2003;254(10):1010-1018. DOI: 10.1016/S0043-1648(03)00307-7

21. ASTM International. *ASTM E3-11(2017) - Standard Guide for Preparation of Metallographic Specimens*. West Conshohocken: ASTM International; 2017. DOI: 10.1520/E0003-11R17

22. Rutherford KL, Hutchings IM. A micro-abrasive wear test, with particular application to coated systems. *Surface and Coatings Technology*. 1996;79(1-3):231-239. DOI: 10.1016/0257-8972(95)02461-1

23. ASTM International. *ASTM G99-17 - Standard Test Method for Wear Testing with a Pin-on-Disk Apparatus*. West Conshohocken: ASTM International; 2017. DOI: 10.1520/G0099-17

24. ASTM International. *ASTM E2546-07 - Standard Practice for Instrumented Indentation Testing*. West Conshohocken: ASTM International; 2007. DOI: 10.1520/E2546-07

25. ASTM International. *ASTM C1624-05 - Standard Test Method for Adhesion Strength and Mechanical Failure Modes of Ceramic Coatings by Quantitative Single Point Scratch Testing*. West Conshohocken: ASTM International; 2005. DOI: 10.1520/C1624-05

26. Verein Deutscher Ingenieure Normen. *VDI 3198*. Dusseldorf: VDI-Verlag; 1991. 8 p.

27. Drescher D, Koskinen J, Scheibe HJ, Mensch A. A model for particle growth in arc deposited amorphous carbon films. *Diamond and Related Materials*. 1998;7(9):1375-1380.

28. Cicek H. Wear behaviors of TiN/TiCN/DLC composite coatings in different environments. *Ceramics International*. 2018;44(5):4853-4858. DOI: 10.1016/j.ceramint.2017.12.074

29. Zaidi H, Djamai A, Chin KJ, Mathia T. Characterisation of DLC coating adherence by scratch testing. *Tribology International*. 2006;39(2):124-128. DOI: 10.1016/j.triboint.2005.04.016

30. Clarysse F, Lauwerens W, Vermeulen M. Tribological properties of PVD tool coatings in forming operations of steel sheet. *Wear*. 2008;264(5-6):400-404. DOI: 10.1016/j.wear.2006.08.031

31. Waseem B, Alam S, Irfan M, Shahid M, Farooq M, Soomro BD, et al. *Optimization and Characterization of Adhesion Properties of DLC Coatings on Different Substrates*. Materialstoday: Proceedings. 2015;2(10 Pt B):5308-5312. DOI: 10.1016/j.matpr.2015.11.041

32. Lara LOC, De Mello JDB. Quantitative measurement of the interface adhesion of a multifunctional coating. *Letters in Applied NanoBioScience*. 2015;4(3):301-305.

33. Lara LC, Costa H, de Mello JDB. Influence of layer thickness on sliding wear of multifunctional tribological coatings. *Industrial Lubrication and Tribology*. 2015;67(5):460-467. DOI: 10.1108/ILT-01-2015-0010